

Using time-lapse analysis to predict reservoir changes in a carbonate pool: a case study of the Rainbow B pool

Hannah T. Tran, Laurence R. Bentley, and E.S. Krebs

ABSTRACT

The Rainbow B pool is a carbonate pool in the process of tertiary production. Miscible gas and solvent were injected into the top of the reservoir in an attempt to extract the remaining oil. The oil in the pore space is being replaced with the gas and the solvent. Two 3D seismic surveys were recorded for the Rainbow B pool. One was acquired in 1987, shortly after the start of tertiary production and the other survey was acquired in 2002. A comparison of the two surveys reveals seismic differences that can be attributed to production-related changes within the reservoir. This will help determine the areas of bypassed oil. Time sags in the seismic data, as well as amplitude changes at the top of the reservoir, reveal areas where gas and solvent were injected.

Before the two surveys can be compared to one another, they must be made to match each other in terms of geometry, time, phase, and frequency. Then subtraction between the two 3D surveys should only reveal production changes. This process is referred to as time-lapse analysis. Preliminary time-lapse analysis in the Rainbow B pool shows the time sags underneath the reservoir, which correspond to the injection zones. However, the amplitude changes at the top of the reservoir are small and poorly correlated to the time sags. The time-lapse analysis results for the Rainbow B pool were also compared to the results the reservoir engineers obtained from simulations with the CMG application. Comparing the geophysical and the engineering results highlight interesting similarities and differences. It was also noted that Gassmann analysis appears to underpredict changes due to solvent and gas substitution.

INTRODUCTION

Generally, time-lapse analysis is mostly used for clastic reservoirs in the North Sea. In Canada, it is mainly utilized for heavy oil projects where steam-assisted drainage is the enhanced oil recovery method. Time-lapse analysis is used to track the location and the direction of the steam front within the reservoir and to detect any bypassed zones. Time-lapse analysis is successfully used for heavy oil projects because the seismic velocities and the densities within the reservoir prior to and after tertiary production are very different, due to steam pressure and temperature greatly affecting fluid and rock properties.

The Rainbow B pool is a carbonate reservoir and the tertiary production method is miscible gas and solvent injection. Time-lapse analysis is not commonly done for carbonate pools because the high bulk modulus of the carbonate greatly exceeds the low bulk modulus of the fluids within the pore space. Thus, the fluid effects seen in seismic data after gas injection are difficult to detect. Hirsche et al. (1998) applied time-lapse analysis on two 2D seismic lines in the Rainbow B pool and discovered that the velocity changes, from pre- to post-tertiary production, are larger than expected. Gassmann analysis appears to underpredict changes. Another case where time-lapse work is being done on a carbonate pool is Weyburn, Saskatchewan, where CO₂ has been injected into the reservoir.

We apply time-lapse analysis to two 3D datasets from the Rainbow B pool acquired in 1987 and 2002. Hampson-Russell's Pro4D application was used to conduct the analysis. By comparing the two seismic datasets, we detected the locations of production-related changes in the reservoir.

This will help determine whether there are areas of bypassed oil or inefficiencies in the production process. First, the 2002 survey is cross-equalized to match the 1987 survey so that the differences due to different acquisition and processing are removed. Then the two surveys are subtracted from one another to detect any differences due to production. The time-lapse analysis results (the geophysical results) are also compared with the engineering results found in the simulation program, CMG.

TIME-LAPSE THEORY

Time-lapse, or 4D, seismic refers to the repetition of a seismic survey after a period of time, — time being the ‘fourth dimension’ — in an effort to image changes that could have occurred in a reservoir. The time-lapse method is useful in that reservoir changes between wells can be detected. It can also be used to improve production, by identifying areas of bypassed oil.

Two or more seismic surveys, acquired at different times but in the same area, are compared to one another to determine whether there are any seismic attribute changes such as traveltimes differences, reflection amplitude differences, or any seismic velocity differences. The differences indicate changes in the reservoir properties. These seismic parameters are directly or indirectly related to the rock properties. Rock physics is used to describe the relationship between the rock properties and the seismic properties. A rock may be described in terms of its elastic parameters: shear modulus (μ), the resistance to shear, and bulk modulus (K), the resistance to compression.

We begin with the basic equations that show the relationship between the seismic velocities and the elastic parameters.

$$V_P = \sqrt{\frac{K + (4/3)\mu}{\rho}}, \quad (1)$$

and

$$V_S = \sqrt{\frac{\mu}{\rho}}, \quad (2)$$

where V_P is the P-wave velocity, V_S is the S-wave velocity, and ρ is the density.

Bulk modulus is affected by a change of fluid within the pore space of a rock but shear modulus is not affected at low frequencies. The change of bulk modulus (K_{sat}), when one pore fluid replaces another pore fluid, is referred to as fluid substitution. The Gassmann (1951) equation (equation (3)) is the most common method used for calculating the effects of fluid substitution (Smith et al, 2003):

$$K_{sat} = K_{dry} + \frac{(1 - \frac{K_{dry}}{K_s})^2}{\frac{\phi}{K_{fl}} + \frac{1 - \phi}{K_s} - \frac{K_{dry}}{K_s^2}}, \quad (3)$$

where K_{sat} is the bulk modulus of a rock saturated with fluids, K_{dry} is the bulk modulus of a dry rock, K_{fl} is the bulk modulus of the fluids, and K_s is the bulk modulus of the solid mineral making

up the rock. Also, ϕ is the porosity. After substitution with a new fluid, a new bulk modulus (K_{sat}) is obtained and a new velocity can be determined.

Two different formulae have been used to compute the bulk modulus of a fluid, giving slightly different results for K_{fl} . They are

$$K_{fl} = S_w K_w + S_o K_o + S_g K_g + S_{sol} K_{sol}, \quad (4)$$

and

$$\frac{1}{K_{fl}} = \frac{S_w}{K_w} + \frac{S_o}{K_o} + \frac{S_g}{K_g} + \frac{S_{sol}}{K_{sol}}, \quad (5)$$

where K_w , K_o , K_g , K_{sol} are the bulk moduli of water, oil, gas and solvent, respectively. S_w , S_o , S_g , S_{sol} are the saturation of water, oil, gas and solvent, respectively. These saturation values are expressed as a fraction of the total fluid content. The sum of the saturation values is 1.

Equation (4) is the arithmetic method, also known as the Voigt average, and equation (5) is the harmonic or the Reuss average. The Voigt method gives the upper bound values while the Reuss method gives the lower bound values. Thus, we will take an average of the upper value and the lower value to determine K_{fl} .

The density also changes when one pore fluid is substituted with another. The density is determined by

$$\rho = \rho_s (1 - \phi) + \rho_{fl} \phi, \quad (6)$$

where ρ_s is the density of the solid mineral making up the rock and ρ_{fl} is the density of the fluids. The density of the fluids is

$$\rho_{fl} = S_w \rho_w + S_o \rho_o + S_g \rho_g + S_{sol} \rho_{sol}, \quad (7)$$

where ρ_w , ρ_o , ρ_g , ρ_{sol} are the densities of the water, oil, gas, and solvent, respectively.

The Batzle and Wang (1992) calculations are used to determine the various values for the fluid densities and for the fluid bulk modulus. The parameters needed for these calculations are pressure, gas gravity, temperature, oil gravity and the gas-oil-ratio.

GEOLOGICAL SETTING

The Rainbow B pool is an atoll reef located in northwest Alberta, township 108-109, range 8 W6M (Figure 1). The map view shows that there is a north lobe and a south lobe. An area referred to as the “saddle point” connects the lobes. The reef is 5.6 km long and 2.1 km wide at its widest point. The average thickness of the reef is 200 m and it is located at a depth of approximately 1800 m. The pool is producing oil from the Middle Devonian Keg River formation. The Keg River formation is overlain by the Muskeg member, which is made of impermeable evaporates, and is underlain by calcareous shales and argillaceous limestones (Figure 2; Hirsche et al., 1998). The depositional environment in the interior of the reef is lagoonal (Figure 3). A lagoonal environment is a quieter setting and therefore lower in porosity than the outer edges of the reef. The average porosity within the B pool is 8% while the average permeability is 460 mD. The majority of the reef is dolomitized. Figure 4 shows a photograph of

core from well 7-10. The main porosity type within the reef is zebroid, intercrystalline and mesovug (Laflamme, 1993).

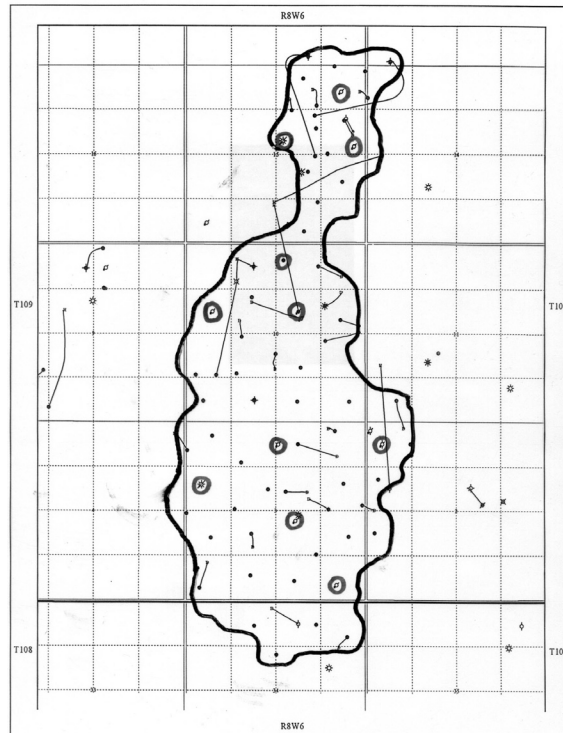


FIG. 1. Rainbow B reef edges. Injection wells are circled.

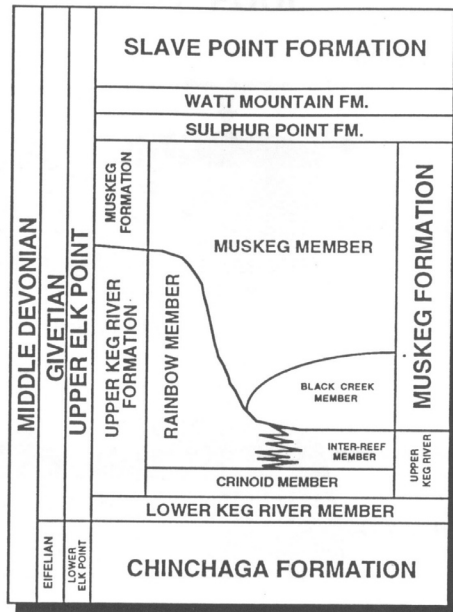


FIG. 2. Stratigraphic chart. The Keg River formation is producing oil. The Muskeg member is the seal (Laflamme, 1993).

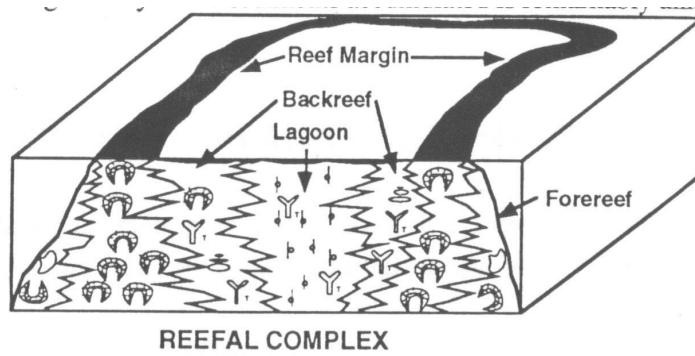


FIG. 3. Model of the Rainbow B reef. The interior of the reef is a quieter lagoonal environment while the reef margin is a higher energy environment. The porosity is higher near the edges of the reef (Laflamme, 1993).



FIG. 4. Core from well 7-10. Porosity type seen here is zebroidal, mesovugs, and intercrystalline. Porosity averages 8%.

Table 1. Rainbow B pool timeline

Date	Process	Description
1965, November	Primary Production	Oil produced by natural drives
1968, March	Secondary Production	Pool waterflooded
1984, June	Tertiary Production	Miscible gas & solvent injection
1987, January	3D seismic data acquired	10 m solvent bank formed
2002, January	3D seismic data acquired	30 m solvent bank formed

RESERVOIR DESCRIPTION

The pool is owned and operated by Husky Energy and has been producing oil since 1965. The original oil in place is $43 \times 10^6 \text{ m}^3$. During primary production, 1.6% of the oil was recovered while 36.5% was recovered during secondary production (Fong et al., 1991). The pressure in the reservoir during production never reached bubble point, which is at 10 845 KPa, so the dissolved gases in the oil did not come out of the solution.

Table 1 shows the timeline for the Rainbow B pool. To further enhance oil recovery, miscible gas and solvent are injected into the top of the reservoir (Figure 5). The solvent helps remove the excess oil from the reservoir and is analogous to dishwashing soap removing grease from a dinner plate. The solvent is injected first and then a lean gas is injected into the reservoir to push the solvent bank down. It is imperative the solvent bank remains horizontal, especially when it reaches the saddle point (Fong et al, 1991). Time-lapse analysis will help determine the injected fluid locations in the reservoir. There are currently 12 injection wells in the reservoir (Injection wells are circled in Figure 1). Table 2 shows some of the reservoir information taken from Nagel et al.'s paper (1990).

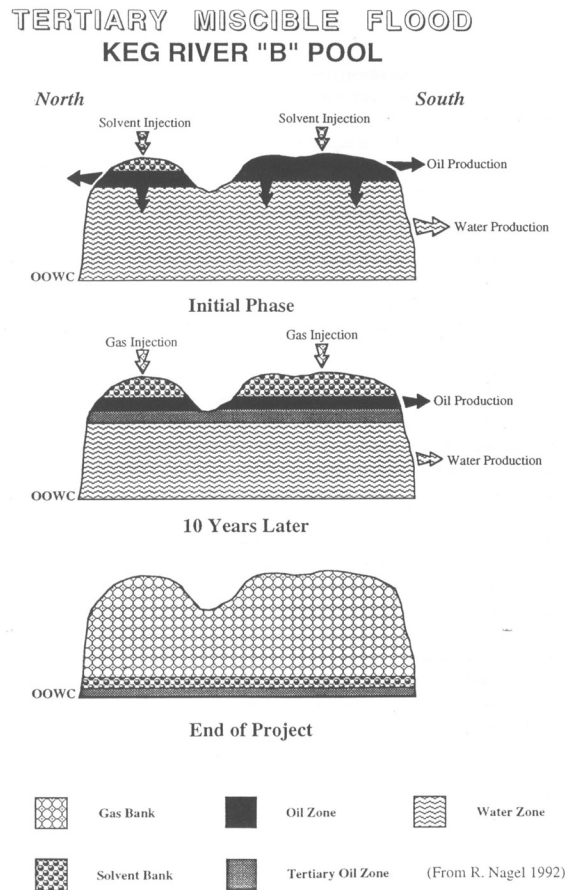


FIG. 5. Tertiary miscible production: The solvent is injected into the top of the reservoir, then the gas is injected to push the solvent bank downwards. During this process, oil and water are produced (Nagel et al., 1990).

Table 2. Reservoir information (Nagel et al., 1990).

Pressure	17.2 MPa
Temperature	87 °C
Original oil in place	43 * 10 ⁶ m ³
Maximum reservoir thickness	233 m
Average oil zone	50 m
Average porosity	8 %
Average permeability	460 mD

THE SEISMIC SURVEYS

Two 3D seismic surveys were acquired. The first survey was acquired in 1987. Gas injection had begun three years previously. An estimated solvent bank of 10 m had formed. Another 3D seismic survey is acquired after fifteen years of further gas injection. The 2002 survey has higher fold than the 1987 survey and the frequency content of the seismic data is also higher. In June of 2002, the 1987 survey was reprocessed so that the processing parameters are the same as the 2002 survey. Also, the 1987 survey has been regridded to the 2002 survey. The in-lines are east-west seismic lines numbered 58 to 350 while the cross-lines are north-south seismic lines numbered 78 to 205 (Figure 6). Figure 6 also shows the time structure map of the top of the Keg River formation (horizon picks are for the 2002 survey). Figure 7 is the isochron map from the Keg River formation to the Cold Lake Formation, which is the high amplitude trough beneath the reservoir. The horizon picks are shown in Figure 8. The Slave Point and the Sulphur Point formation are picked as a peak and the Keg River and the Cold Lake formation are picked as a trough. Figure 8 shows a north-south cross section (cross-line 130) of the south lobe of the pool and from data acquired in 1987. The 2002 survey along the same cross-section is shown in Figure 9. Note that the frequency content of the 2002 seismic data is higher than in the 1987 survey. Also, only the seismic traces within the Rainbow B pool are presented because the seismic traces around the pool have been removed due to confidentiality. Some of the processing parameters are listed in Table 3.

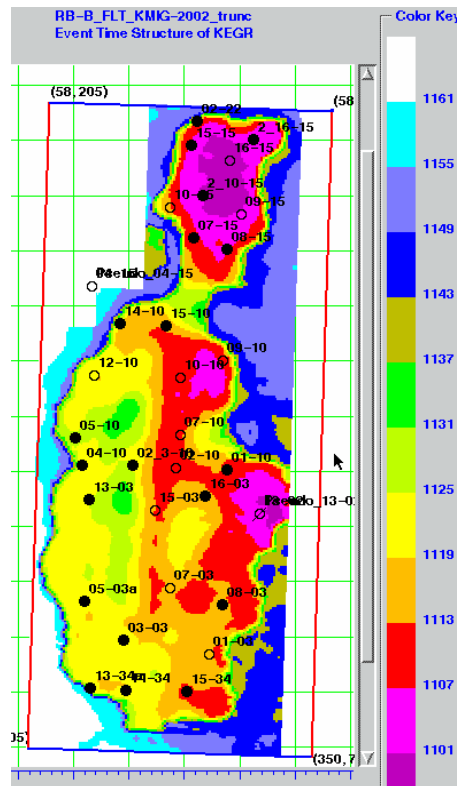


FIG. 6. Time structure of the top of the Keg River (units in milliseconds).

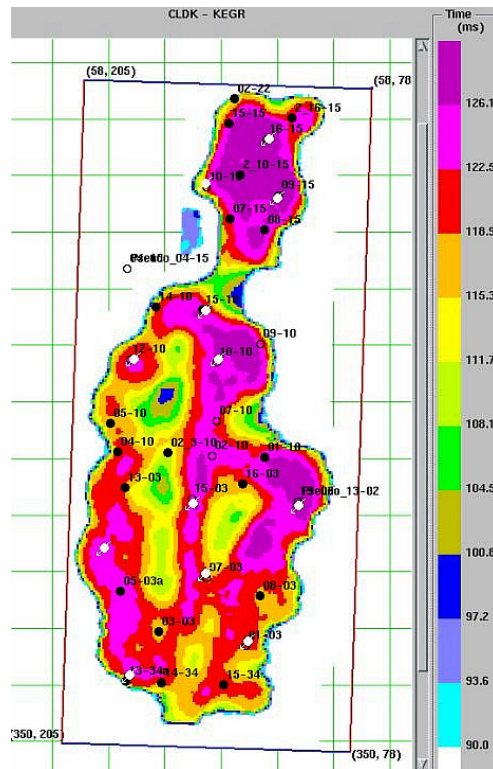


FIG. 7. Isochron of Keg River to Cold Lake.

Table 3. Parameters for the 3D seismic surveys.

1987 survey	2002 survey
Acquired Dec 31, 1986 to January 25, 1987	Acquired February 12-20, 2002
Re-processed October 2002	Processed June 2002
20 m bin size	20 m bin size
Datum: 550 m; Replacement velocity: 2500 m/s	Datum: 550 m; Replacement velocity: 2500 m/s
Pre-stack Kirchoff migration	Pre-stack Kirchoff migration
Filter: 8-12-90-110 Hz	Filter: 8-12-90-110 Hz
but original filter was 4-8-70-80 Hz	

CROSSEQUALIZATION RESULTS

Crossequalization is the industry term for time-lapse processing, which is the processing used to match the poststack seismic data sets. Before the two seismic data sets could be compared, they have to be crossequalized to match one another in terms of acquisition geometry, phase, time or static correction, frequency, and amplitude. In general, a wavelet operator is estimated to shape and match the reflection data of one survey to another (Ross et al., 1996). The crossequalized trace is calculated by convolving the input trace by the wavelet operator based on phase, time, frequency, and amplitude. Then the two seismic datasets can be subtracted from one another to find the differences that are likely to be due to the production effects.

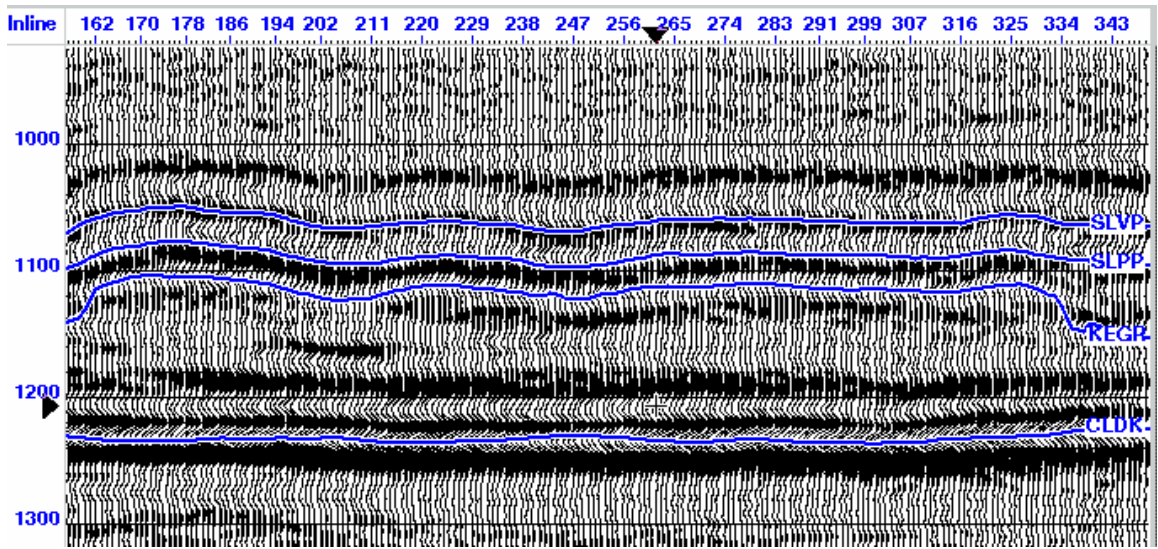


FIG. 8. 1987 seismic data (Base survey), southern lobe. Cross-line 130; SLVP = Slave Point; SLPP = Sulphur Point; KEGR = Keg River; CLDK = Cold Lake.

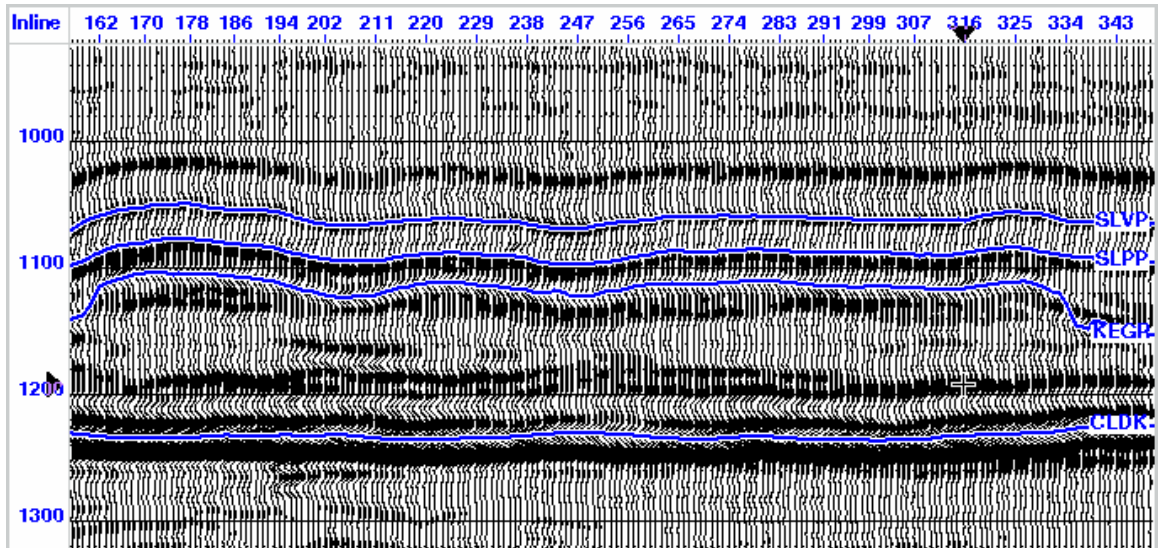


FIG. 9. 2002 seismic data (Monitor survey), Cross-line 130. Note higher frequency content than the 1987 survey.

The newer survey (2002) is sometimes referred to as the MONITOR survey and the older survey (1987) as the BASE survey. The Base seismic data are lower in frequency than the Monitor seismic data so it is better to crossequalize the Monitor data so that it matches the Base data. We do not recommend crossequalizing the Base data to match the Monitor data because this may introduce high-frequency noise into the Base data. The crossequalization procedure consists of:

1. Regridding
2. Phase- & time-shifting
3. Applying shaping/matched filter
4. Crosscorrelation shallow statics/"Warping": used to interpret time differences
5. Time-variant shifts: used to interpret amplitude differences

Step 1 — Regridding

Regridding matches the processing output geometry of one seismic survey to the other. Kelman Processing reprocessed the two 3D datasets so that they have the same in-line and cross-line names. The datasets also have the same replacement velocity and the same datum.

Step 2 — Phase- and time-shifting

The next step is phase- and time-shifting, which estimates and applies a first-order constant-phase correction and a constant bulk time-shift. The time shift will vary with respect to the phase shift. To overcome this problem, both the time shift and the phase shift are estimated together via the Russell-Liang technique. To determine the time shift in this technique, a time-pick is made on the envelope amplitude of the crosscorrelation of the Base to the Monitor survey. To determine the phase shift, a pick is made on the instantaneous phase of crosscorrelation (between the two surveys) that corresponds to the time of the envelope maximum (Pro4D course). In normal cases, windows are usually chosen to include the reservoir. Then a correlation threshold is applied so that the seismic traces within the production zone are not used to estimate the phase and time shift. In my case, I do not have seismic traces around the pool and so I have to use a window above the reservoir. Since there should be no production effects above the reservoir, the Monitor seismic data above 1100 ms should be made to match the Base data as closely as possible. The window chosen to estimate the corrections is between 750-1100 ms, which is above the reservoir. A global average-matching process is used so that there is only one phase- and one time-shift applied to all the traces. The global average matching process is better than the trace-by-trace process because the global option insures that the trace-by-trace variations are preserved (F. Ma, personal communication, 2002). The results show that a first-order phase shift of -19.3 degrees and a time shift of -2.44 ms were calculated and applied.

Step 3 — Applying shaping filter

The shaping filter step (also referred to as match filtering) derives and applies a shaping filter to the Monitor survey. This process is used to match the static time-shift, the phase, the amplitude and the frequency content between the surveys by calculating a convolutional shaping filter based on a certain design window (Rickett et al., 2001). This shaping filter step uses the Wiener-Levinson filtering algorithm. The Wiener shaping filter operator is derived by using the crosscorrelation lags of the Base survey to the Monitor survey, and using the autocorrelation lags

of the Monitor survey (Yilmaz, 1987). Then the Wiener shaping filter is convolved with the Monitor survey. Again, a window from 750-1100 ms is used and the processing used is the global average method.

Step 4 — Crosscorrelation shallow statics

Crosscorrelation shallow statics applies a time shift that is derived from crosscorrelation analysis. This procedure has also been referred to as applying a “warp”, used to align mispositioned events (Rickett et al., 2001). This procedure is different from the phase- and time-shift step because that step is not able to spatially position reflectors due to differences in NMO and migration velocity functions between the two surveys (Ross et al., 1997). Also, this procedure calculates the time shift by the trace-by-trace method rather than by the global average method. The window is designed above the zone of interest. Thus after this calibration step, the seismic data above the zone of interest should be the same in both data sets since there is an assumption that there are no production effects there. A time sag can be detected below the areas where gas and solvent were injected. This is because the replacement of oil with gas and solvent cause a velocity decrease in the reservoir.

Figure 10 shows how the Monitor data look after phase and time shifting, having a shaping filter applied and after cross-correlation shallow statics. The coloured areas on the figure (near 1230 ms) represent the subtraction of the monitor data after crossequalization versus the monitor data before crossequalization. The subtraction of the crossequalized monitor data and the Base survey is shown in Figure 11. The high amplitude events at 1230 ms (the Cold Lake horizon) indicate the biggest differences. The time sags underneath the production zones are shown clearly at 1230 ms because the Cold Lake is a strong event. These time sags are consistent with areas where gas and solvent have been injected. The 1987 survey is crosscorrelated to the crossequalized 2002 survey from a window of 1200-1250 ms. The time shift required to match the Cold Lake horizons on the Base and the crossequalized Monitor survey is represented in map view (Figure 12). The purple colours are interpreted as locations in the reservoir where gas and solvent were injected.

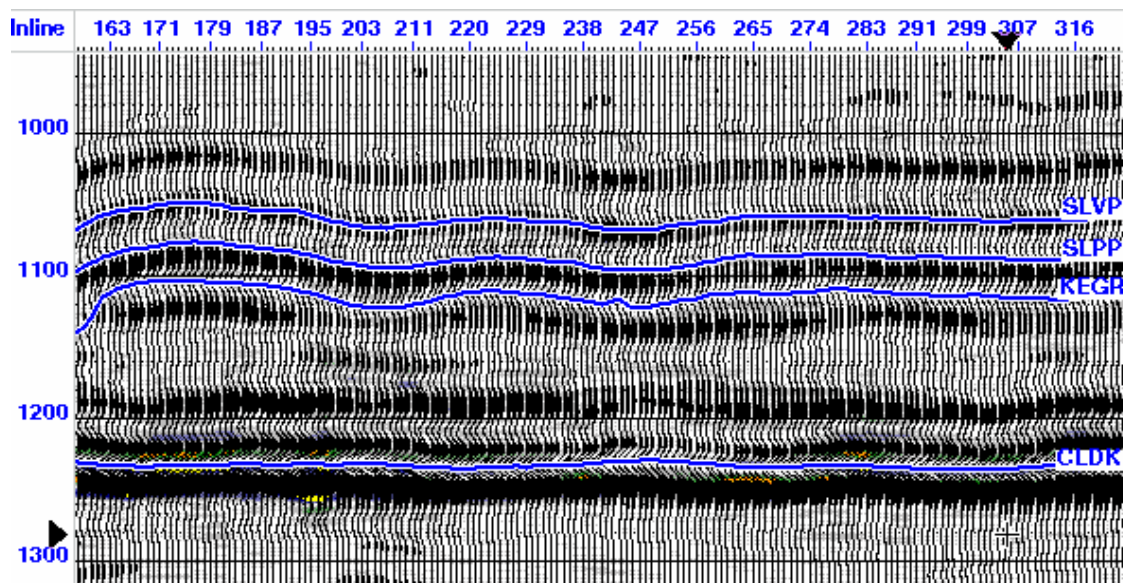


FIG. 10. 2002 seismic data, crossequalized to match the Base survey (after applying steps 1–4); crossline 130; Colours shown near the Cold Lake horizon represent the differences between the Monitor data and the crossequalized Monitor data.

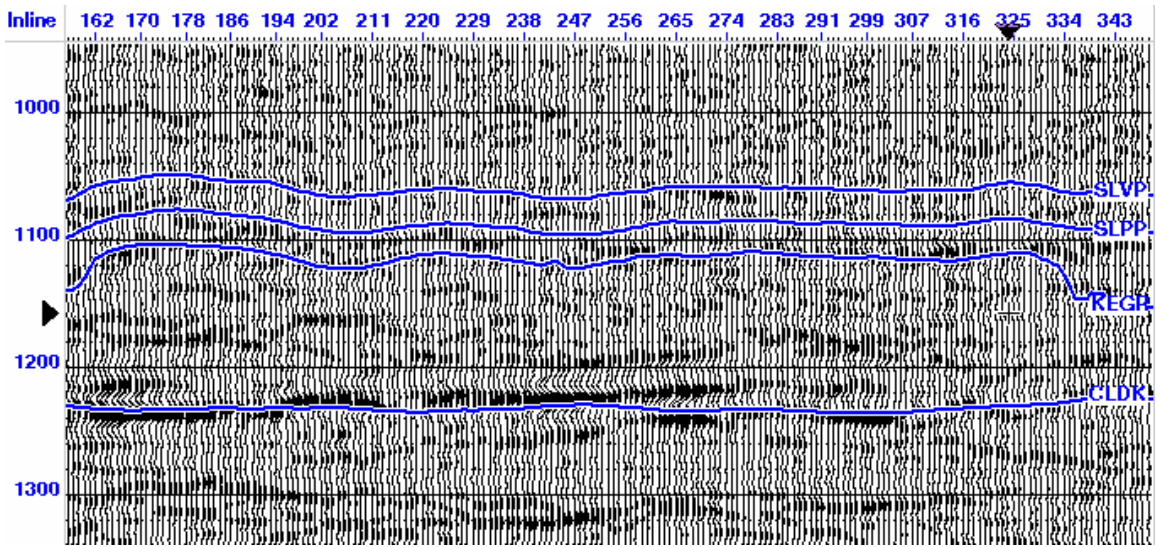


FIG. 11. Difference between the 1987 survey and the crossequalized 2002 survey (after applying steps 1–4). High-amplitude events at the Cold Lake horizon are due to time sags beneath the production zones.

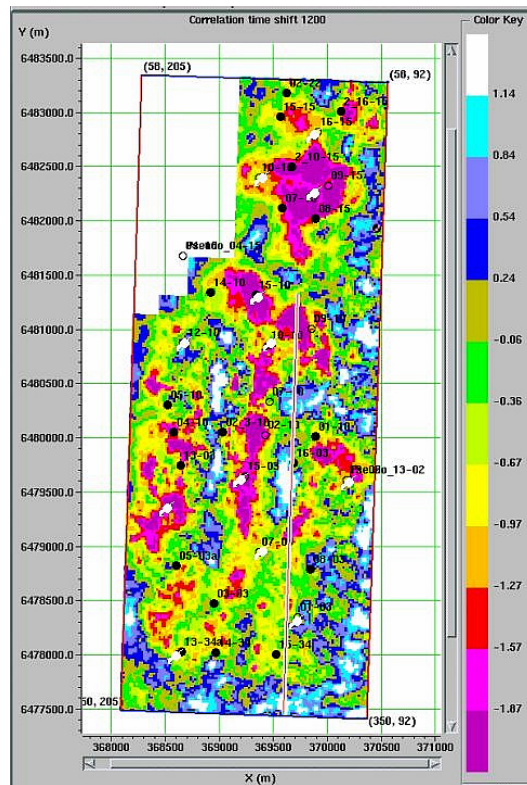


FIG. 12. Time-shift map for a window at 1200-1250 ms (centred on the Cold Lake horizon). Purple areas represent the time sags in the reservoir. These time sags are due to the replacement of oil with gas and solvent.

Step 5 — Time-variant shifts

The last calibration step is to apply time-variant shifts, which is similar to the procedure in the previous step except that two windows are required, one above and one below the reservoir. Thus, two time-shifts are derived from the crosscorrelation analysis and the time shifts between the two windows are interpolated. This step attempts to match the Base and Monitor data in terms of time, above, within, and below the reservoir. After time deficiencies have been minimized, amplitudes can be compared. The Base and the crossequalized Monitor survey (after applying the phase and time-shifting step, the shaping filter step, the crosscorrelation shallow static step, and the time variant shifts step) are subtracted. A map of the RMS amplitude differences, which has been normalized to the average amplitude of the input surveys, is shown in Figure 13. A window of 20 ms is centred at the Keg River horizon. The replacement of oil with gas would cause the reflection amplitudes at the top of the Keg River to increase from the Base survey to the crossequalized Monitor survey. The purple areas in Figure 13 may be interpreted as areas where there is gas found near the top of the reservoir.

CMG SIMULATION RESULTS

CMG is a computer program used by the reservoir engineers to do reservoir simulation and history matching. This simulation is used to help predict the reservoir properties in the future and to determine how long it will take for the hydrocarbons to be depleted. A specific program within CMG, called Results3D, displays the results of the simulation. It is used to visualize the reservoir. The Rainbow B pool was split into different sized grid blocks. There are 25 columns, 60 rows, and 41 layers. The map of layer 13 illustrates the porosity distribution (Figure 14).

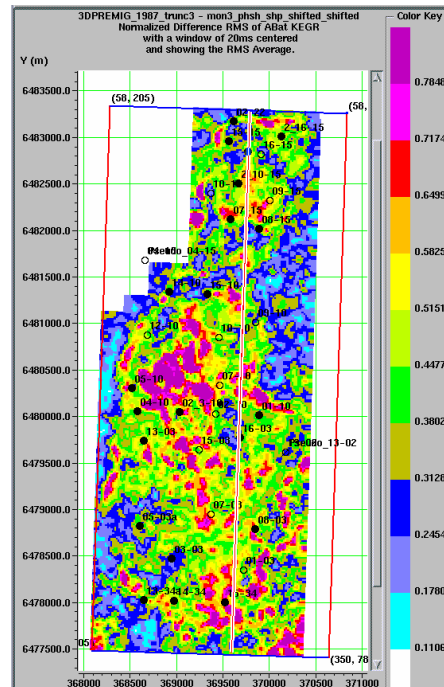


FIG. 13. Normalized RMS averaged amplitude map of the difference section with a window centred at 20 ms on Keg River. The purple represents the amplitude changes at the top of the reservoir due to the presence of gas and solvent. This map does not correlate well with the time-shift map in Figure 12.

Porosity data were taken from the geological information at the well locations and they were interpolated between the wells. The north lobe has higher porosity and also the edges of the reef have higher porosity than the interior.

Figure 15 shows a north-south cross-section (column 16) of the fluid contacts from the simulation results in January of 1987. The grid blocks that are mostly saturated with water are in light blue. The green colours represent the grid blocks that are mostly saturated with oil while red represents the grid blocks with both gas and solvent. Figure 16 is the same cross-section for the year 2002. There is more gas and solvent injected and most of the water has been produced. The thickness of the gas- and solvent-saturated grid blocks in Figure 15 and 16 can also be represented in map view (Figure 17). The grid block thicknesses are summed up over the layers saturated with gas and solvent. Then the difference is taken of the total thickness between 1987 and 2002.

The volume of gas and solvent in the reservoir between the period 1987 and 2002 can also be determined. Each grid block has a different porosity value and different saturation values for the water, oil, gas and solvent. These saturation values all add up to one. Also, each grid block has a different thickness, th . The volume of fluid in each grid block is found by multiplying the saturation times the porosity times the layer thickness. For example, Equation 8 is used to determine the volume of gas (Vol_g) in each grid block.

$$Vol_g = (S_g)(\phi)(th) \tag{8}$$

At each horizontal location, the volumes of gas in each grid block could be added together vertically to give Vol_{total_g} . Then take the difference between Vol_{total_g} in 1987 and in 2002 to determine how much gas has been injected during this time. The same calculations are done to determine the solvent that has been injected in that period. The replacement of oil with either gas or solvent causes a time sag in the seismic data. The map showing the sum of the volume of gas and of solvent injected between 1987 and 2002 is displayed in Figure 18. More gas and solvent has been injected in the north lobe.

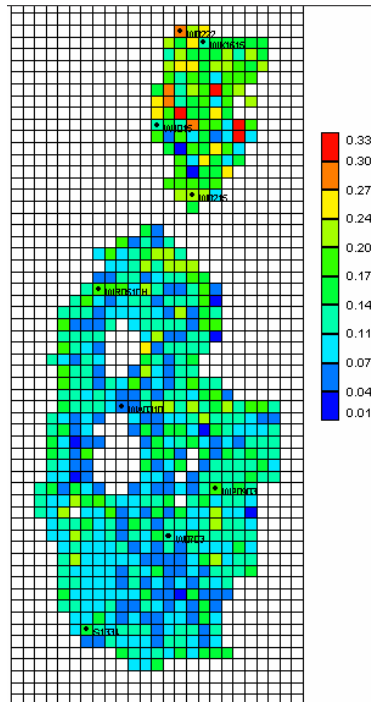


FIG. 14. Map view of the porosity in layer 13. Note high porosity in the north lobe and higher porosities on the edges of the reef. (from CMG results).

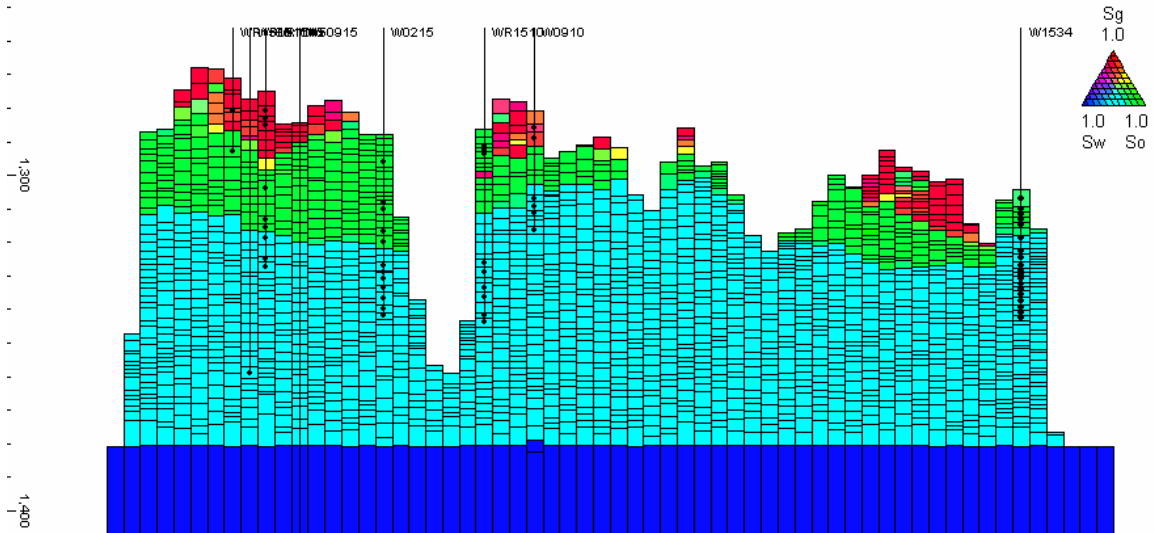


FIG. 15. North-south cross-section of the fluid contacts in 1987-01-01. Light blue represents the grid blocks saturated with mainly water. Green represents the oil-saturated grid blocks. Red represents the gas- and solvent-saturated grid blocks.

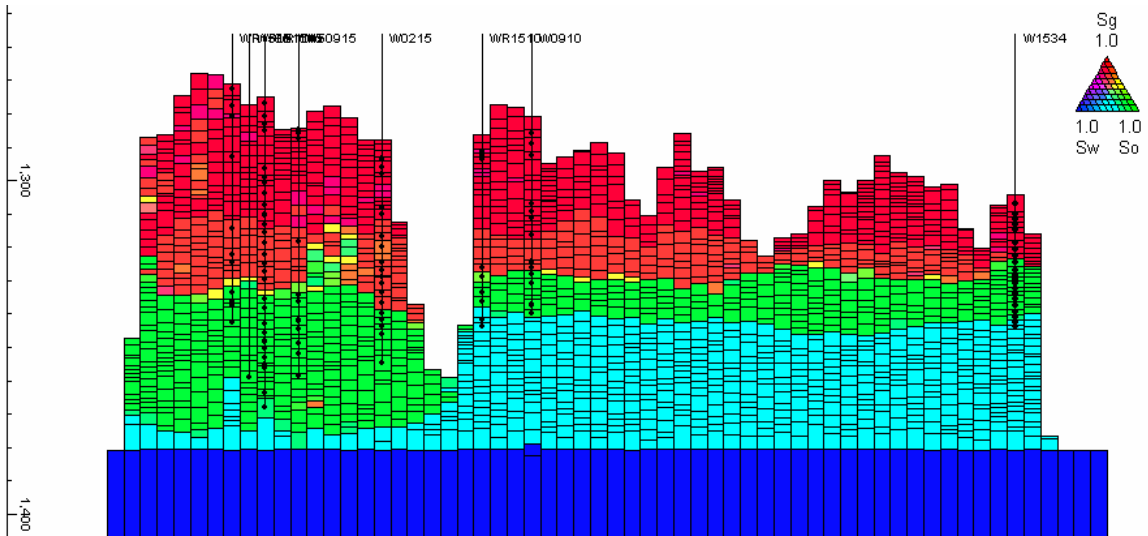


FIG. 16. North-south cross-section of the fluid contacts in 2002-01-01. Light blue represents the grid blocks saturated with mainly water. The oil-saturated grid blocks are green. The gas- and solvent-saturated grid blocks are red.

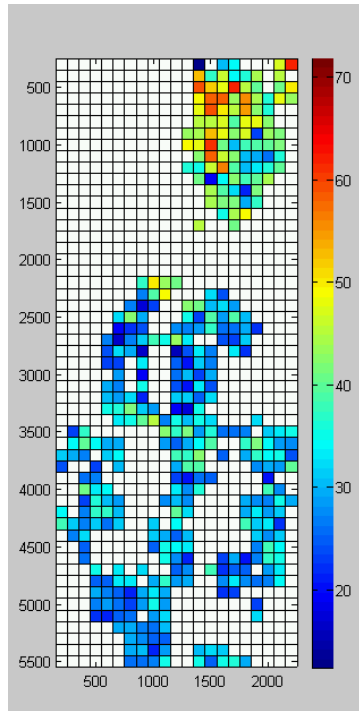


FIG. 17. Difference between the 1987 and the 2002 gas- plus solvent-saturated grid block thickness summed over the layers (units are in metres).

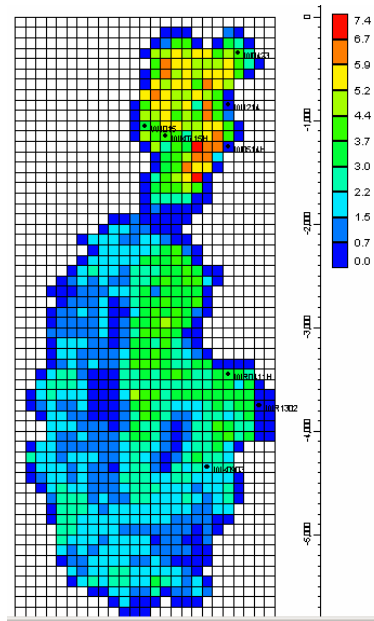


FIG. 18. Difference between the 1987 and the 2002 gas-plus-solvent volumes summed over all the layers [(gas saturation * porosity * thickness of the grid block) + (solvent saturation * porosity * thickness of the grid block)]; units are in metres.

HAND CALCULATIONS

Figure 18 shows model results of changes of gas-plus-solvent volumes at different locations within the reservoir, but it is not directly comparable to the seismic data because the results are not in time. The Gassmann equation is used to calculate the bulk modulus, which is used to determine the velocity, which is used to determine the time sag.

Step 1. — Find K_{dry} for each grid block

The velocity from equation (1) is needed to determine the time-shifts. There are no dipole sonic logs in this field. However, some cores from wells 15-3 and 15-15 were tested in the laboratory by Husky for the V_p/V_s ratio. The V_p/V_s ratio is related to μ by rearranging equations (1) and (2):

$$V_p = \sqrt{\frac{K_{dry} + \frac{4}{3} \left(\frac{K_{dry}}{A - (4/3)} \right)}{\rho}}, \quad (10)$$

where $A = (V_p/V_s)^2$.

From laboratory tests on the cores of wells 15-3 and 15-15, the V_p/V_s ratio for a dry rock is 1.79 while the dry rock V_p is measured to be 5219 m/s. The density of dolomite is known to be 2870 kg/m^3 and the dry rock density is $2870 \cdot (1 - \phi)$. The porosity, ϕ , from the CMG results is different for each grid block and so different K_{dry} values are calculated. After putting the values into equation 10 yields K_{dry} to be an average 40 GPa.

Step 2 — Determine K_{sat} for each grid block.

$$K_{sat} = K_{dry} + \frac{(1 - \frac{K_{dry}}{K_s})^2}{\frac{\phi}{K_{fl}} + \frac{1 - \phi}{K_s} - \frac{K_{dry}}{K_s^2}}$$

K_{sat} values are calculated from the Gassmann equation (equation (3), repeated above). ϕ values are from the CMG results. K_s for dolomite is 94.9 GPa (Mavko et al, 2000). K_{dry} values have been calculated and stored in CMG. The Batzle and Wang calculations determine the bulk modulus of the water, the oil, the gas and the solvent. Then these values are used in equations (4) and (5) to calculate K_{fl} . The input and the output results for the Batzle and Wang calculations are shown in Table 4 and 5.

Table 4. Fluid input values for the Batzle and Wang calculations

Pressure (MPa)	Gas Gravity	Temperature (°C)	Oil Gravity	Gas Oil Ratio	Solvent Gravity
17	0.683	87	39	79.78	1.13

Table 5. Fluid output values from the Batzle and Wang calculations

	Water	Oil	Gas	Solvent	Dolomite
Density (g/cc)	0.9832	0.7279	0.1272	0.293	2.87
Bulk modulus (GPa)	2.5005	0.6771	0.0334	0.056	94.9

Step 3 — Calculate the velocity

$$V_p = \sqrt{\frac{K_{sat} + \frac{4}{3} \left(\frac{K_{sat}}{A - (4/3)} \right)}{\rho}} \quad (11)$$

Density (ρ) values are calculated from equations (6) and (7). The porosity values are from CMG and the density values of the individual fluids are from the output of the Batzle and Wang calculations. “A” is assumed to be the same as above.

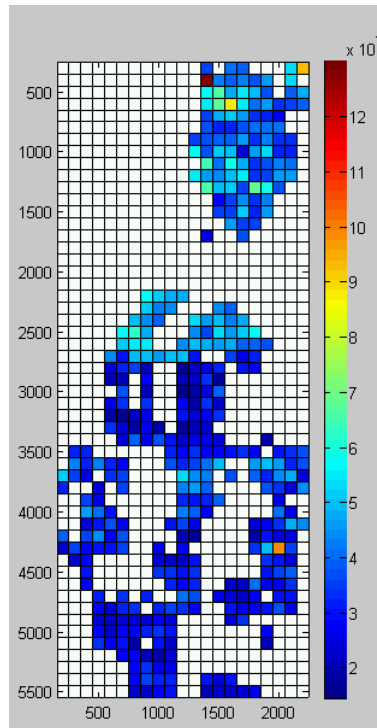


FIG. 19 Time sags (units of ms) calculated based on saturation and porosity results from CMG simulation. These results are also based on the Gassmann calculations and the Batzle and Wang calculations.

Step 4 — Find the time to travel through each grid block

Each grid block in CMG will have a different velocity. The traveltimes through each of these grid blocks is determined by dividing the thickness of the grid block by its velocity. The original traveltimes through the blocks are subtracted from the new traveltimes and then multiplied by two to account for two-way traveltime. The traveltime differences are summed for each location and the results are plotted in Figure 19. Figure 18 shows the volume of injected fluid but it does not show the results in time; Figure 19 does. The traveltime differences are very small compared to the results found after crossequalization in the seismic data. This is because the Gassmann equation underestimates the velocity differences from the Base survey to the Monitor survey. One way to overcome this problem is to increase the fluid bulk modulus of the water and the oil (Hirsche et al, 1998).

DISCUSSION

Figures 12 and 19 can be compared because both represent traveltime differences. Figure 12 shows the geophysical results based on subtracting the calibrated Monitor survey from the Base survey. The time sags are shown in purple and they correspond to the injection wells. Figure 19 shows the calculated results (from the Batzle and Wang equations and the Gassmann equations) based on the various fluid saturation values and porosities that are used in the CMG simulation. Both the engineering data and the geophysical data show that there is fluid injected into the north lobe of the reservoir.

Time-lapse analysis is useful because it obtains information in between the wells. However, there are some limitations to this study. First of all, the Base survey should have been acquired prior to tertiary production. Instead, it was done three years after gas and solvent injection began. Therefore, it is harder to interpret the results of the locations of where the gas and the solvent are suspected to be in the reservoir. Secondly, the 1987 survey is poor in frequency content but the 2002 survey has to be crossequalized to match the 1987 survey. Therefore, the time-lapse seismic results are also poor in frequency content. Thirdly, the seismic traces around the pool have been removed. This makes it harder to confirm that the differences within the pool are correct compared with the differences around the pool. Lastly, carbonate reservoirs are usually thought to be bad candidates for time-lapse analysis. The time-shifts obtained were less than 3 ms. Nonetheless, although the shifts were small, they were still anomalous and show where the injection wells are.

CONCLUSIONS

Preliminary time-lapse analysis has been presented for the Rainbow B pool, a carbonate reservoir. The results show the zones where gas and solvent were injected. The 2002 survey was crossequalized to match the 1987 survey. After applying crosscorrelation time-shift, the time sags beneath the zone of injected fluids are revealed. After applying time-variant shift, the RMS amplitude differences at the top of the Keg River are found to be small and poorly correlated with the time sags. The geophysical time-lapse results and the results from the CMG simulation have similarities and differences. Both the seismic and the simulation results show that the north lobe has a thick bank of injected fluids. Another similarity is that the central part of the south lobe also has a thick bank of injected fluids. There are a few places where the simulation results show locations of injected gas but the seismic data does not. Another difference is that when the simulation is converted to time, the time sags are much smaller than the time-lapse analysis results show. Gassmann analysis appears to underpredict changes due to solvent and gas substitution. Overall, time-lapse analysis seems to work better and for more case studies than we expected (I. Jack, personal communication, 2003).

FUTURE WORK

An inversion will be performed on the seismic data to enable a more direct interpretation of the results. The fifth crossequalization step, the time-variant shift step, will be repeated with sliding and overlapping windows rather than with only two windows in an attempt to improve the amplitude differences. Calculations will also be repeated in an attempt to get the simulation results in time closer to the seismic results, perhaps by increasing the fluid modulus of the water and the oil by a certain factor. Also, time-lapse modelling will be compared to the time-lapse results. Since differences in pressure could also cause velocity changes, the pressure in the reservoir will be analyzed. Also, the seismic results will be quantitatively compared to the CMG results. Finally, more detailed interpretations will be performed.

ACKNOWLEDGEMENTS

Thanks to Husky Energy for the data; Larry Mewhort, who helped us tremendously in supplying data and suggestions; Ken Hedlin, for his suggestions; Andre Laflamme, for showing us the cores; Husky B Pool Asset Team Engineers and Geologists, for the CMG simulation results. At the University of Calgary, thanks for support from the CREWES Project, and to Ying Zou and John Zhang. At Hampson-Russell, thanks to Francis Ma.

REFERENCES

- Batzle, M., Wang, Z., 1992, Seismic properties of pore fluids: *Geophysics*, **57**, 1396-1408.
- Fong, D.K., Wong, F.Y., Nagel, R.G., Peggs, J.K., 1991, Combining a volumetric model with a pseudo-miscible field simulation to achieve uniform fluid leveling in the Rainbow Keg River 'B' Pool: *Journal of Canadian Petroleum Technology*, **30**, 65-76.
- Gassmann, F., 1951, Uber die elastizitat poroser medien: *Verteljahrss-chrift der Naturforschenden Gesellschaft in Zurich*, **96**, 1-23.
- Hirsche, K. and Hirsche, J., 1998, Seismic monitoring of gas injection and solvent floods in carbonate reservoirs: unpublished for Western Geophysical.
- Laflamme, A.K., 1993, "B" pool reservoir characterization pilot study (section d): Carbonate Technical Group Geological Report (unpublished?)
- Mavko, G., Mukerji, T., Dvorkin, J., 1998, *The Rock Physics Handbook – Tools for seismic analysis in porous media*: Cambridge Univ. Press.
- Nagel, R.G., Hunter, B.E., Peggs, J.K., Fong, D.K., Mazzocchi, E., 1990, Tertiary application of a hydrocarbon miscible pool: Rainbow Keg River "B" pool: *SPE Reservoir Engineering*, 301-378.
- Rickett, J.E., Lumley, D.E., 2001, Crossequilization data processing for time-lapse seismic reservoir monitoring: A case study from the Gulf of Mexico: *Geophysics*, **66**, 1015-1025.
- Ross, C.P., Altan, M.S., 1997, Time-lapse seismic monitoring: Some shortcomings in nonuniform processing: *The Leading Edge*, **16**, 931-937.
- Ross, C.P., Cunningham, G.B., Weber, D.P., 1996, Inside the crossequilization black box: *The Leading Edge*, **14**, 1233-1240.
- Smith, T.M., Sondergeld, C.H., Rai, C.S., 2003, Gassmann fluid substitutions: a tutorial: *Geophysics*, **68**, 430-440.
- Wang, Z., 2001, Fundamentals of seismic rock physics: *Geophysics*, **66**, 398-412.
- Yilmaz, O., 1987, *Seismic Data Processing*: Society of Exploration Geophysicists